Effect of the excited states on the disappearance of the dynamical interference from the atomic two-photon ionization

Haiying Yuan(袁海颖)[1], Shushan Zhou(周书山)[2], Susu Zhang(张稣稣)[3], Jigen Chen(陈基根)[4], Jun Wang(王俊)[3], Fuming Guo(郭福明)[3*] and Yujun Yang(杨玉军)[3**]

[1]School of Physics and Electronic Engineering, Jining University, Qufu 273155, Shandong, China

[2]School of Physics and Electronic Technology, Liaoning Normal University, Dalian 116029, China

[3]Institute of Atomic and Molecular Physics, Jilin University, Changchun 130012, China

[4]Zhejiang Provincial Key Laboratory for Cutting Tools, Taizhou University, Jiaojiang 31800, China

September 11, 2026

Abstract

By solving the three-dimensional time-dependent Schrödinger equation accurately, the ionization process of a hydrogen atom under the action of a laser pulse with a frequency of 0.3 a.u. was investigated. The study revealed that with the increase of the driving laser intensity, the ionization probability of the atom declined after rapidly increasing, exhibiting a characteristic of ionization suppression. It is noteworthy that the dynamic interference disappears in a certain range of laser intensities in the ionization suppression zone. Through the analysis of the excited state of the system, it is found that the reason for the disappearance of the dynamic interference phenomenon is that in addition to the direct ionization of electrons from the ground state, there is also the excitation to the excited state first and then ionized from the excited state, the laser intensity for which has not yet reached the ionization suppression requirement in the meantime.

Keywords: above-threshold ionization, excited states, ionization suppression

PACS: 32.80.Rm, 42.50.Hz

1. Introduction

With the progress of laser technology, especially the development of high harmonic generation [1–6] and free electron laser techniques, it has become possible to experimentally obtain a coherent light source at high frequencies (including XUV and X-ray bands) [7–11]. The interaction between these light sources and atoms can lead to ionization [12–18]. Generally, it is expected that the ionization probability would increase with the laser intensity. However, ionization studies of the interaction of high-frequency laser fields with atoms have revealed a counter-intuitive phenomenon, in which the ionization rate of atoms in high-frequency laser fields decreases with increasing laser intensity above a critical value. This phenomenon is

*Corresponding authors. Email: guofm@jlu.edu.cn; yangyj@jlu.edu.cn

known as atomic stabilization [19–22], and it has been experimentally observed through the ionization of Rydberg atoms [23–27].

The understanding of the stabilization phenomenon is usually explained using Floquet theory: the ionization suppression is related to the generation of eigenfunctions of the electronic wave function or the Kramers-Henneberger potential during the interaction process. Under the Kramers-Henneberger transformation, for a single-frequency laser field, the time-dependent motion of the electron can be transformed into an eigenvalue problem. However, for ultrashort high-frequency laser pulses, this model is no longer valid and requires dynamic analysis [28]. For the single-photon ionization process, the electronic ionization from the atom under the condition of a high-frequency laser pulse at lower intensities mainly occurs throughout the entire pulse duration. With the increase of the laser intensity, the ionization suppression process is generated, and atomic ionization primarily appears during the rising and falling edges of the laser pulse. The distribution of ionized electrons can exhibit subpeak structures due to the coherence of ionized electrons from different moments [29]. The generation of this interference structure is typically regarded as a signature of ionization suppression. Baghery *et al*. studied photoelectron emission from single photon ionization and found that dynamic interference can occur during the ionization of the excited state of the hydrogen atom, but not during the ionization of the ground state of the hydrogen atom [30]. Jiang *et al*. clearly observed the pattern of dynamic interference on the photoelectron spectrum of ionization of the ground state of the hydrogen atoms and did not confirm the results of Baghery *et al*., and the study also pointed out that the atom stabilization phenomenon is closely related to dynamic interference [31].

Ionization suppression has also been investigated for the two-photon ionization process. Su *et al*. found suppression of two-photon ionization of atoms by one-dimensional numerical simulations [32]. Pont *et al*. used circularly polarized laser pulses to interact with hydrogen atoms and ionization suppression was proved for the ionization of the atoms as the enhancement of the laser intensity [33]. Under non-ionization suppression conditions, Müller *et al*. investigated the influence of laser pulse intensity with a frequency of 0.375 a.u. on the hydrogen atom's photoelectron emission spectrum. The presence of resonant transitions from the ground state to the 2p state, when the pulse intensity is high enough to induce the Rabi oscillation, results in a distinct multi-peak structure in the photoelectron emission spectrum, which is further explained by the dynamic interference [34]. However, the effect of ionization suppression on the photoelectron emission spectrum in the case of two-photon ionization was not discussed in these works.

In this paper, the effect of excited states on the photoelectron emission spectrum in the case of two-photon ionization suppression was discussed. We have investigated the ionization process of a laser pulse with a frequency of 0.3 a.u. interacting with a hydrogen atom by numerically solving a time-dependent Schrödinger equation (TDSE) scheme, and observed a clear ionization suppression phenomenon. Under a certain laser condition for ionization suppression, it is found that the photoelectron emission spectrum does not show a clear dynamic interference structure and this phenomenon is caused by the ionization of the electron transfer to the excited state. The ionization suppressed laser intensity of the ground state and different excited states are different, so the photoelectron emission spectrum does not show clear dynamic

interference structure due to the interference from different ionization channels.

2. Theoretical Methods

In order to study the photoelectron emission process of atoms under the action of a laser electric field, it is necessary to numerically solve the time-dependent Schrödinger equation. Usually based on the coordinate space, after the atom is ionized by the laser pulse, the ionized electrons will move far away from the nuclear region, the calculation requires a lot of space and a very large number of grid points for obtaining the convergence result. Therefore, in this paper, the time-dependent generalized pseudospectral (TDGPS) method of the momentum space is used to solve the time-dependent Schrödinger equation of the system [35,36]. This scheme can obtain accurate calculation results, and at the same time reduce the requirements for computing resources. Under the dipole approximation and velocity gauge, the time-dependent Schrödinger equation in momentum space is (Unless otherwise specified, atomic units are used in the paper):

$$i\frac{\partial}{\partial t}\Phi(\mathbf{p},t)=\left[\frac{\mathbf{p}^2}{2}+\frac{1}{c}\mathbf{A}(t)\cdot\mathbf{p}\right]\Phi(\mathbf{p},t)+\int V\left(\mathbf{p},\mathbf{p}'\right)\Phi\left(\mathbf{p}',t\right)d\mathbf{p}', \tag{1}$$

The Coulomb potential of the momentum space is defined as

$$V\left(\mathbf{p},\mathbf{p}'\right)=\frac{1}{(2\pi)^3}\int U(\mathbf{r})\exp[i(\mathbf{p}'-\mathbf{p})\cdot\mathbf{r}]d\mathbf{r}. \tag{2}$$

For the hydrogen atom, the Coulomb potential is

$$V\left(\mathbf{p},\mathbf{p}'\right)=-\frac{1}{2\pi^2}\frac{1}{\left|\mathbf{p}-\mathbf{p}'\right|^2}. \tag{3}$$

The momentum space potential is expanded in partial waves as

$$V\left(\mathbf{p},\mathbf{p}'\right)=\frac{1}{pp'}\sum_{l=0}^{l_{\max}}\sum_{m=-l}^{l}V_l\left(p,p'\right)Y_{lm}(\theta,\phi)Y_{lm}^{*}\left(\theta',\phi'\right), \tag{4}$$

where $p=|\mathbf{p}|$, $l_{\max}$ is the maximum number of the partial waves used in the calculation, $Y_{lm}(\theta,\varphi)$ is the spherical harmonics, and

$$V_l\left(p,p'\right)=-\frac{1}{\pi}Q_l\left(\frac{p^2+p'^2}{2pp'}\right). \tag{5}$$

Here, Q_l is Legendre function of the second kind [37].

If the linearly polarized laser field is along z direction, the time-dependent wave function $\Phi(p,t)$ is expanded in the partial waves as [38,39]

$$\Phi(\mathbf{p},t)=\frac{1}{p}\sum_{l=0}^{l_{\max}}\varphi_l(p,t)Y_{l0}(\theta,\phi), \tag{6}$$

where, $\varphi_l(p,t)$ is the momentum space radial wave function. Applying Eqs. (4) and (6) to Eq. (1), we can obtain an integro-differential equation for the momentum space radial wave function

$$\begin{aligned}i\frac{\partial}{\partial t}\varphi_l(p,t) &= \frac{p^2}{2}\varphi_l(p,t)+\int V_l(p,p')\varphi_l(p',t)dp' \\ &\quad +\frac{1}{c}pA(t)[\alpha_{l+1}\varphi_{l+1}(p,t)+\alpha_l\varphi_{l-1}(p,t)],\end{aligned} \tag{7}$$

where $\alpha_l = \frac{l}{\sqrt{(2l-1)(2l+1)}}$.

There is a logarithmic singularity in the potential $V_l(p,p')$ [40]. To remove this singularity, the Landé 's subtraction technique is used [41]. A singularity-free TDSE is obtained for the radial wave function after removing the singularity.

To solve the singularity-free TDSE, the TDGPS method [42] is extended to the momentum space computation [43]. The momentum space domain $[0,\infty]$ is mapped to a new finite domain $[-1,1]$ by a mapping function

$$p(x) = \gamma \frac{1+x}{1-x+x_m}. \tag{8}$$

where γ is a mapping parameter chosen as 1.8, and $x_m = 2\gamma/p_{max}$ with the maximum momentum $p_{max} = 2$ a.u. The smaller the value of γ, the denser the grid points at small momentum p.

By projecting the continuum state on the time-dependent wavefunction at the end of the laser pulse, one can obtain the continuum state and the corresponding single differential cross section is

$$\frac{dP_\varepsilon}{d\varepsilon} = \sum_l |b_l(\varepsilon, t_{fin})|^2. \tag{9}$$

where t_{fin} is the end moment of the laser pulse and $b_l(\epsilon,t)$ is continuum state population amplitude.

The population of bound states is produced by projecting the wave function of the system at the end of the laser pulse onto the bound states

$$p_{n,l}(t) = \left|\langle \psi_{n,l}(\mathbf{p}) \mid \Phi(\mathbf{p},t)\rangle\right|^2. \tag{10}$$

By calculating the population of bound states, the ionization probability of the system can be determined

$$p_{\text{ion}} = 1 - \sum_{n,l} p_{n,l} \tag{11}$$

3. Results and Discussion

We used the laser vector potential in the form of $A(t) = \frac{cE_0}{\omega} f(t)\sin(\omega t+\phi)$ and the electric field in the form of $E(t) = -\frac{\partial A(t)}{c\partial t}$, where E_0 represents the peak amplitude of the laser electric field, ϕ is the carrier envelope phase (CEP) of the incident laser pulse, we set $\phi = 0$. Here, $\omega = 0.3$ a.u.is the frequency of the incident laser pulse, $f(t)$ is the pulse envelope function, when $0 < t < \frac{2\pi\tau_R}{\omega}$, $f(t) = \sin^2(\frac{\omega t}{2\pi\tau_R})$, elsewhere $f(t) = 0$. The duration of the laser pulse is about $\frac{\tau_R}{2}T$ (T is the optical cycle, o.c.) and chosen to be 15 o.c.. Figure 1(a) gives the variation of atomic ionization probability with the peak electric field amplitude of the driving laser pulse. From the figure, the atomic stabilization phenomenon can be observed, i.e., with the increase of the peak electric field amplitude, the ionization probability of atoms is enhanced, and reaches the maximum value when the peak amplitude of the electric field is 0.144 a.u. (here, the strength of the electric field where ionization suppression occurs is referred to as the ionization suppression critical electric field strength E_{cri}), and then with the further enhancement of the peak amplitude of the laser electric field, the ionization probability of atoms no longer increases but rather decreases.

Figure 1(b) presents the photoelectron emission spectra at peak electric field amplitudes E_0 of 0.1 a.u., 0.15 a.u., 0.2 a.u., and 0.3 a.u., which corresponds to peak amplitudes at a, b, c, and d in Fig.1(a). From this figure, it can be found that the photoelectron emission spectrum shows a single-peak structure when $E_0 = 0.1$ a.u.. In the ionization suppression region, i.e. E_0 is greater than 0.144 a.u., the width of the photoelectron emission peak at $E_0 = 0.15$ a.u. is wider than that in the case of $E_0 = 0.1$ a.u. and some traces of the interference structure are seen. It is worth noting that when $E_0 = 0.2$ a.u., the photoelectron emission spectrum appears to have a single peak rather than a multi-peak structure, as $E_0 = 0.3$ a.u., the photoelectron emission spectrum has a multi-peak structure. To better understanding of this photoelectron emission spectrum feature, we systematically investigated the photoelectron emission spectra of different peak amplitudes of the laser electric field.

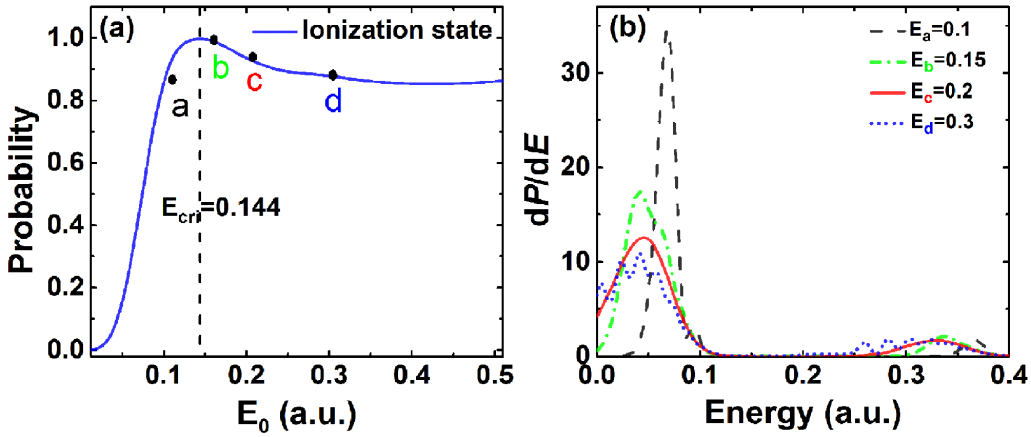


Fig. 1. (a) The total ionization probability of a hydrogen atom as a function of the peak amplitude of the laser electric field. (b) Photoelectron emission spectra at peak amplitudes E_0 of 0.1 a.u., 0.15 a.u., 0.2 a.u., and 0.3 a.u..

Figure 2 displays the change of the photoelectron emission spectra with the peak amplitude of the incident laser electric field. From the figure, it can be seen that the first photoelectron peak is mainly caused by the ionization of electrons absorbing two photons from the ground state. When the peak electric field amplitude is small, the energy of the photoelectron peak is 0.1 a.u., which satisfies $2 \times 0.3 - I_p$. As the increase of the peak amplitude of the laser field, the energy of the ionization peak decreases (e.g., at the black dashed line in Fig. 2) because of the AC-Stark effect of the driving laser, and the position of the energy of the peak can be determined with the energy conservation equation $E_k = n\omega - I_p - U_p$ (I_p is the ionization energy, $U_p = E_0^2/4\omega^2$ is the ponderomotive energy acquired by the electron) [44]. The main peak of the photoelectron emission spectrum is a single peak structure. When the peak amplitude of the laser electric field is large enough, ionization suppression occurs, and the energy position of the first photoelectron peak is near 0, which is characterized by a multi-peak structure (e.g., $E_0 = 0.3$ a.u. in this figure). However, it is worth noting that, when E_0 is greater than E_{cri}, the photoelectron emission peaks in the region (the white dashed box in the figure) are still single-peak structures, and the multi-peak structure of dynamic interference in the photoelectron emission spectrum is not observed. In contrast,

when E_0 is further enhanced, the photoelectron emission spectra show the multi-peak structure of dynamic interference. As can be found from Fig. 2, in the ionization suppression region, the photoelectron emission spectra for E_0 from 0.16 a.u. to 0.23 a.u. do not show a clear dynamic interference structure, which requires an in-depth analysis of its generation mechanism.

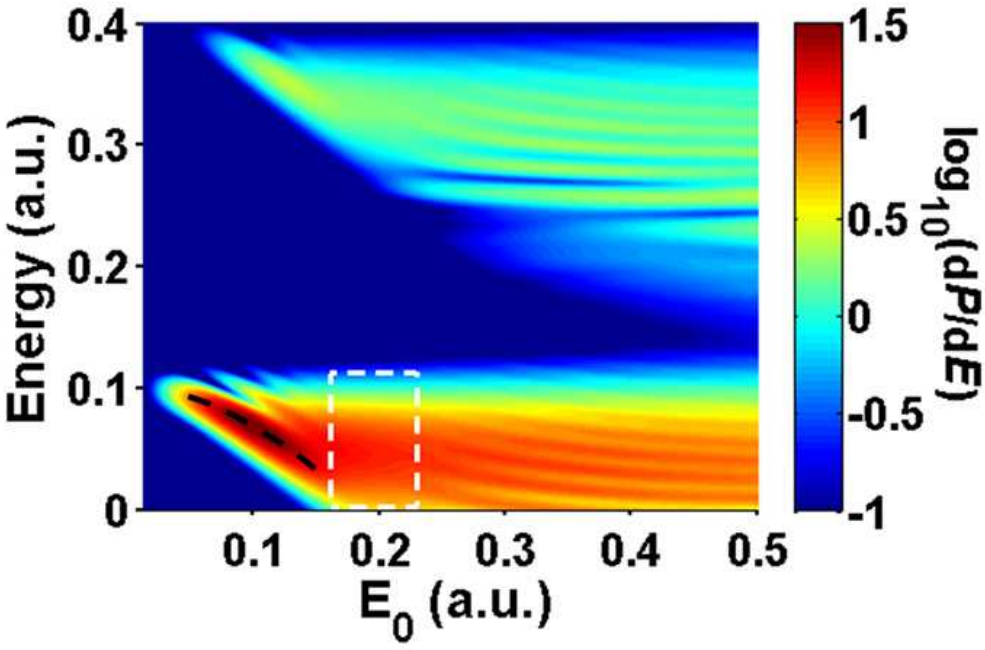


Fig. 2. Photoelectron emission spectra of a hydrogen atom as a function of the peak amplitude of the incident laser electric field.

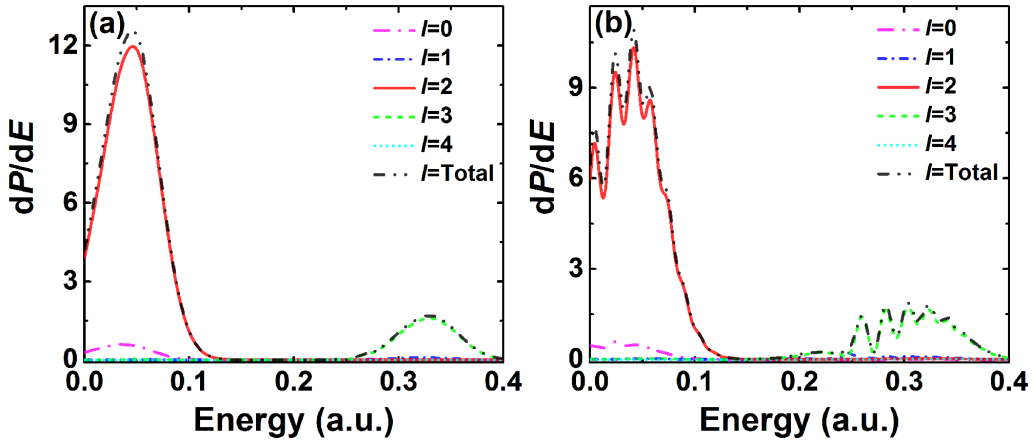


Fig. 3. (a) Partial wave photoelectron spectra of the hydrogen atom at an incident laser electric field peak amplitude of 0.2 a.u. and (b) partial wave photoelectron spectra of the hydrogen atom at an incident laser electric field peak amplitude of 0.3 a.u..

In the following, we checked the partial wave photoelectron emission spectra of hydrogen atoms in electric field with peak amplitudes of 0.2 a.u. and 0.3 a.u., as shown in Figs. 3(a) and (b), respectively. As can be seen from the figures, the photoelectron emission peak is a single-peak structure when $E_0 = 0.2$

a.u., and the photoelectron emission spectrum shows a multi-peak structure as $E_0 = 0.3$ a.u.. It can be found that the $l = 2$ partial wave mainly contributes to the first photoelectron emission peak. According to the angular momentum conservation, the ionization of electrons requires an even number of photons. Meanwhile, according to energy conservation, the ionization of electrons requires two photons under the action of the laser pulse with a frequency of 0.3 a.u.. The $l = 3$ partial wave accounts for the major contribution in the second photoelectron emission peak. Due to angular momentum conservation, the ionization of electrons needs to absorb an odd number of photons. At the same time, electrons need to absorb three photons for ionization because of energy conservation. Such photoelectron production is possible either by direct photon ionization of electrons absorbing photons from the ground state, or by electrons jumping from the ground state to the excited one and then being ionized. To prove this mechanism, we analyzed the excited state's population of the atom at the end of the laser pulse.

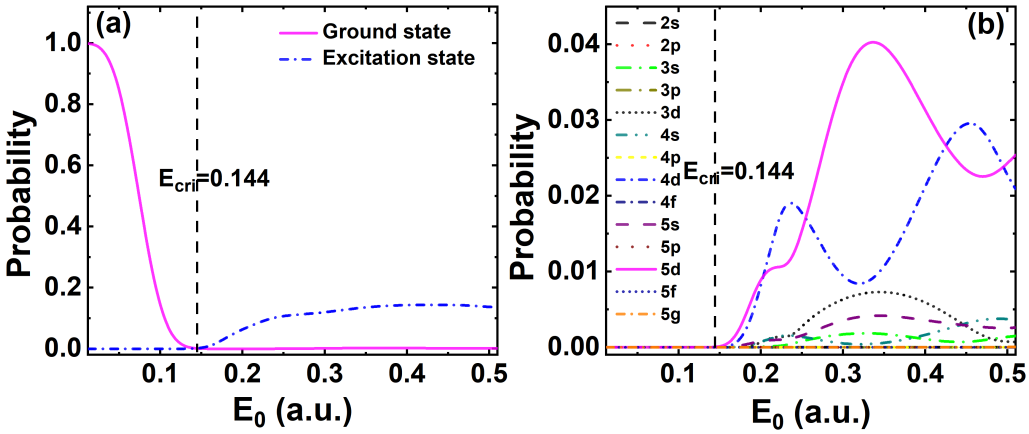


Fig. 4. (a) Ground state population and total excited state population as a function of the peak amplitude of the incident laser field. (b) Excited state populations as a function of the peak amplitude of the incident laser field.

Fig. 4(a) presents the variation of the populations of the ground and total excited states with the peak amplitude of the electric field at the end of the laser pulse. From the figure, with the increase of the peak electric field amplitude, it can be seen that the ground state population decreases rapidly between $E_0 = 0$ a.u. and $E_{cri} = 0.144$ a.u., while the total excited state population of the system is unchanged and the population is almost zero. The ground state population is almost depleted when the peak amplitude of the incident laser electric field is larger than that of ionization suppression critical field strength $E_{cri} = 0.144$ a.u.. Moreover, the excited state population increases significantly and reaches 0.15 a.u. at the end of the laser pulse. Therefore, one can deduce that ionization suppression does not occur when the peak electric field amplitude is represented by the vertical dashed line in Fig. 4(a), but only the ionization reaches the maximum value, and the photoelectron emission peaks generated by the peak electric field amplitude can be mainly observed. With further increase of the peak amplitude of the laser field, the generation of a multi-peak structure of the photoelectron emission spectrum associated with the ionization suppression can usually be observed, such as at the peak amplitude of the electric field of 0.3 a.u. in the Fig.2. In

contrast, due to the effect of the excited state, we observed the generation of only single-peak structures in the peak electric field amplitude range of 0.16 a.u.-0.23 a.u..

To verify the above conjecture, we further investigated the variation of the populations of more bound states $2s$, $2p$, $3s$, $3p$, $3d$, $4s$, $4p$, $4d$, $4f$, $5s$, $5p$, $5d$, $5f$, and $5g$ states with the peak amplitude of the electric field at the end of the laser pulse, as shown in Fig. 4(b). From the figure, it can be found that when $E_0 > E_{cri}$, the populations of the $5d$ and $4d$ states are relatively large compared to those of the other states. To further test the inference that the single peak in the photoelectron emission in the ionization suppression region may be related to the excited state, we then calculated the photoelectron emission spectra when the initial state is the excited state.

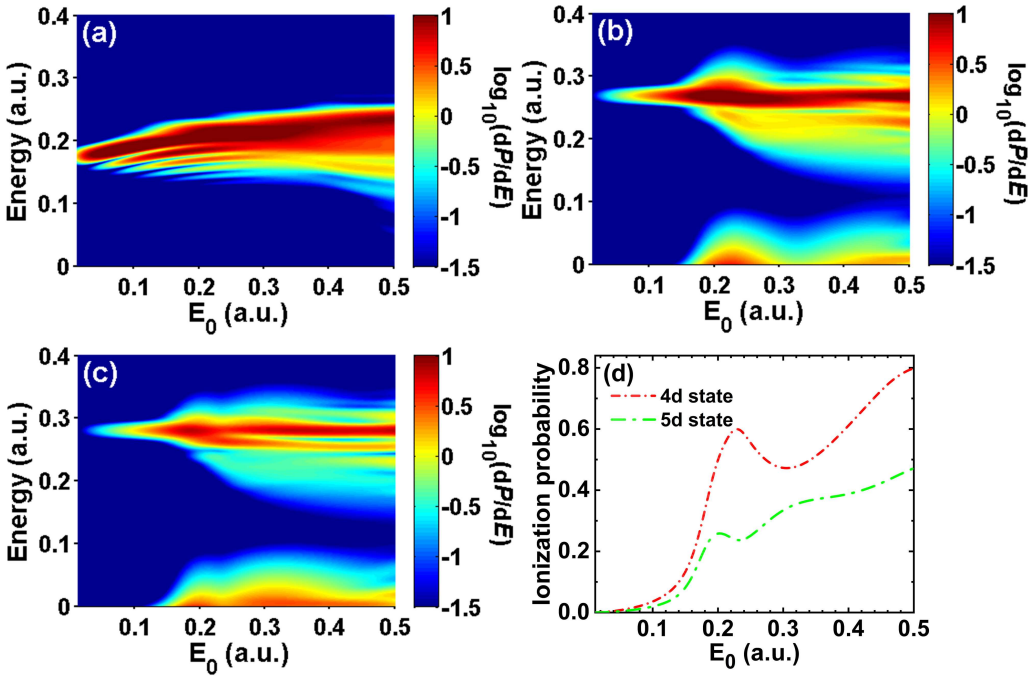


Fig. 5. Photoelectron emission spectra from the initial (a) $2p$, (b) $4d$, and (c) $5d$ states as a function of the peak amplitude of the incident laser electric field. (d) Ionization probabilities from the initial $5d$ and $4d$ states as a function of the peak amplitude of the incident laser electric field.

Since the $2p$ state energy level is more likely to resonate with the $1s$ initial state to produce resonance excitation followed by ionization, we next investigated the photoelectron emission spectra when the initial state of atoms is $2p$, $4d$ and $5d$ states under the same laser parameters, as shown in Figs. 5(a)-(c). From Fig. 5(a), it can be found that when the $2p$ state is the initial state, there is almost no photoelectron emission peaks near the energy of 0 in the photoelectron emission spectrum. Instead, the energy position of the first photoelectron emission peak is near 0.2 a.u., which does not overlap with the photoelectron emission spectrum near energy 0 in Fig. 2. Therefore, the photoelectrons in this energy range are not from the ionization of electrons in the $2p$ state. However, in Figs. 5(b) and (c), it can be found that, when the $5d$ and $4d$ states are the initial states, the generated photoelectron emission spectra produce significant peaks near the energy position of 0, which overlap with the energy position of the first photoelectron

emission peak near 0 in Fig. 2. As a result, the reason for the disappearance of the dynamic interference is not the influence of the 2p state but the excited nd (n>3) state. The photoelectron emission spectra from the higher excited states such as 6d, 7d, etc. are similar to those of the 4d and 5d states as the initial state, and results for the 4d and 5d states are presented here. The roles of higher-lying excited d states and a more detailed analysis are provided in the supplementary material.

From Figs. 5(b) and (c), it can be found that, especially when the peak amplitude exceeds 0.2 a.u., the corresponding ponderomotive energy is very large. Consequently, the photoelectron spectra for both the 4d and 5d excited states as initial states show a single peak structure. With the enhancement of the peak electric field amplitude, the width of the photoelectron emission peaks in the photoelectron emission spectra becomes broader, and the multi-peak structure of dynamic interference appears, which changes from one main peak to multiple peaks. Combined with the analysis of Fig. 2, it can be found that the first photoelectron emission peak is shifted below the threshold due to the shift of the ponderomotive energy. The electron absorbs two photons population onto discrete states d states which are just below threshold. It continues to absorb a third photon ionized to an energy position near 0.3 a.u., which is the mechanism that generates the 2nd photoelectron emission peak. Since this mechanism cannot contribute to the photoelectron peak near the energy of 0, the 2nd photoelectron emission peak is accompanied by the stimulated emission of one photon near this peak, the depopulation of which induces the photoelectron emission peak near the energy of 0. The appearance of photoelectron emission peaks near energy 0 from Figs. 5(b) and 5(c) also indicate the occurrence of the above physical process.

We further investigated the ionization probability of the atom with the initial state of $5d$ state and $4d$ state with the peak amplitude of the laser field, as shown in Fig. 5(d). As can be observed from the figure, with the increase of the peak amplitude of the incident laser electric field, the ionization probability of the initial $5d$ state gradually increases and the ionization rate reaches the maximum when the peak amplitude of the electric field is 0.2 a.u., and then decreases instead of increasing. For the $4d$ initial state, the ionization probability gradually increases with the increase of the peak amplitude of the incident laser field and reaches a maximum when the peak amplitude of the incident laser electric field is 0.23 a.u., and then begins to decrease. Therefore, in the electric field peak amplitude range of 0.16 a.u.-0.23 a.u., the reason for the single peak in the ionization suppression region in Fig. 2 is due to the effect of the excited state when the excited state is the initial state, it doesn't belong to the ionization suppression region, which thus leads to a single-peak structure generated by the ionization from the ground state.

Based on understanding the mechanism of the excitation effect on the low-energy photoelectron emission, we further analyzed the effect of excited states under different laser peak amplitude conditions. In the following, we calculated the change of the ground state population of the system with time and analyzed the change of the photoelectron emission spectrum under the condition of constant ground state population. We first simulated the change of ground state population of hydrogen atoms with time for peak amplitudes of the electric field of 0.1 a.u., 0.2 a.u., and 0.3 a.u., as shown in Figs. 6(a), 6(d), and 6(g). The horizontal axis of the figure represents time, and the color represents the variation of the intensity

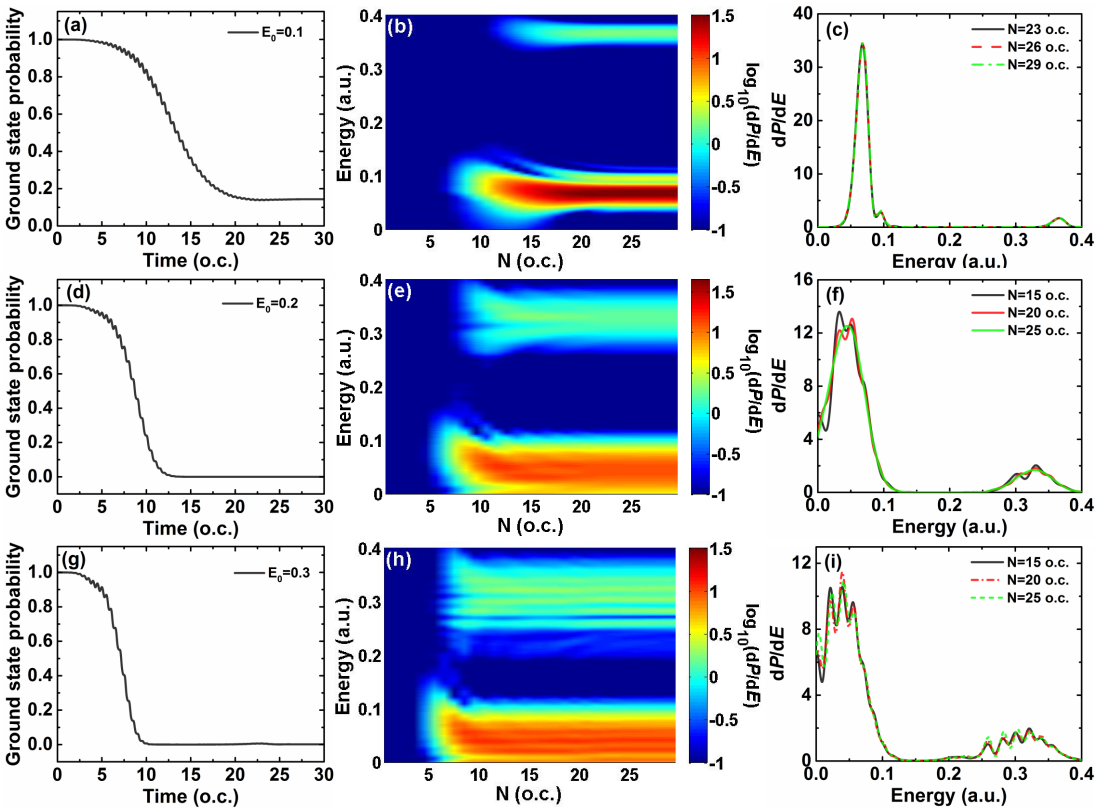


Fig. 6. Time evolution of the ground state population of hydrogen atoms for different laser field peak amplitudes: (a) peak amplitude of 0.1 a.u., (d) peak amplitude of 0.2 a.u., and (g) peak amplitude of 0.3 a.u.. The photoelectron emission spectra produced by the coherent superposition of the ionized electron wave packets at each cycle from 0 to N optical cycles (N=1, 2, 3...30) for different peak amplitudes: (b) peak amplitude of 0.1 a.u., (e) peak amplitude of 0.2 a.u. and (h) peak amplitude of 0.3 a.u.. Furthermore, (d), (f), and (i) show the photoelectron emission spectra resulting from the coherent superposition of ionized electrons within 23 optical cycles, 26 optical cycles, and 29 optical cycles for a peak amplitude of 0.1 a.u.; 15 optical cycles, 20 optical cycles, and 25 optical cycles for a peak amplitude of 0.2 a.u.; and 15 optical cycles, 20 optical cycles, and 25 optical cycles for a peak amplitude of 0.3 a.u., respectively.

of the photoelectron emission spectrum obtained by coherent superposition of the electron wave packets ionized in each optical cycle from time 0 to N optical cycles.

Through detailed comparison, it was observed that when the electric field peak amplitude is 0.1 a.u., as depicted in Fig. 6(a), the ground state population decreases with increasing time, and after the 22nd optical cycle, it remains constant. Meanwhile, from Fig. 6(b), it can be noted that the photoelectron energy spectrum resulting from the coherent superposition of ionized electrons after 22 optical cycles is consistent with the spectrum generated at the end of the laser pulse, and the main peak is a single-peak structure. To understand clearly the impact of excited states on the photoelectron emission spectrum in the time range, during which the ground state population remains constant, we provided the photoelectron emission spectra resulting from the coherent superposition of ionized electrons in each optical cycle within 23, 26, and 29 optical cycles, as presented in Fig. 6(c). It is evident from the figure that the photoelectron emission spectra from ionized electrons within 23, 26, and 29 optical cycles are nearly identical because the excited state has no effect on the photoelectron emission spectrum at this time.

When the electric field peak amplitude is 0.2 a.u., as shown in Fig. 6(d), the ground state population rapidly decreases with increasing time and stabilizes after the 12th optical cycle. Meanwhile, Fig. 6(e) reveals that the photoelectron emission spectrum resulting from the coherent superposition of ionized electrons from 6 to 20 optical cycles exhibits a multi-peak structure, differing from the spectrum generated at the end of the laser pulse. However, the photoelectron emission spectrum resulting from the coherent superposition of ionized electrons after 20 optical cycles is consistent with that produced at the end of the laser pulse. Therefore, it is due to the appearance of a new ionization channel after 20 optical cycles that the dynamic interference phenomenon in the photoelectron emission spectrum disappears and becomes a single-peak structure. In the following, we displayed the photoelectron emission spectra resulting from the coherent superposition of ionized electrons within 15, 20, and 25 optical cycles, as shown in Fig. 6(f). From this figure, it can be found that the photoelectron emission spectra resulting from the coherent superposition of ionized electrons within 15 and 20 optical cycles exhibit a multi-peak structure, while the spectrum within 25 optical cycles turns into a single-peak structure. At this point, the contribution of excited states leads to a single-peak structure in the photoelectron emission spectrum.

When the electric field peak amplitude is 0.3 a.u., as exhibited in Fig. 6(g), the ground state population rapidly decreases with increasing time and stabilizes after the 10th optical cycle. From Fig. 6(h), it can be noticed that the photoelectron emission spectrum resulting from the coherent superposition of ionized electrons in the time range of 6 to 30 optical cycles is a multi-peak structure. To see more clearly the effect of the excited state on the photoelectron emission spectra when the ground state fabrication is kept constant. We provided the photoelectron emission spectra resulting from the coherent superposition of ionized electrons within 15, 20, and 25 optical cycles, as shown in Fig. 6(f). From the figure, it can be found that the photoelectron emission spectra obtained by coherent superposition of ionized electrons in each optical cycle within 15, 20, and 25 optical cycles are multi-peak structures with obvious differences. It can be reflected that the excited state still has an influence on the photoelectron emission spectrum at

this time.

4. Conclusion

In summary, by numerically solving the time-dependent Schrödinger equation scheme, this paper theoretically and systematically investigated the ionization process of the hydrogen atom irradiated by laser pulses with a frequency of 0.3 a.u.. It is found that as the peak amplitude of the incident laser electric field increases, its ionization probability enhances to a certain value and then decreases, and the phenomenon of ionization suppression occurs. When the driving laser electric amplitude reaches the laser intensity conditions in the region of dynamic ionization stabilization, a single-peak structure is observed in the photoelectron emission spectrum. This structure is analyzed and demonstrated to be produced by the effect of the electron in the ground state jumping to the excited states. This study shows that one can modulate photoelectron emission under few-photon ionization conditions through the excited states.

Acknowledgements. Project supported by the National Key Research and Development Program of China (Grant No. 2019YFA0307700), National Natural Science Foundation of China (NSFC) (Grants No. 12074145, No. 11774129, No. 11975012, No. 12204214 and No. 12374029); Jilin Provincial Research Foundation for Basic Research, China (20220101003JC), Outstanding Youth Project of Taizhou University (Grant No. 2019JQ002) and project ZR2024QA074 supported by Shandong Provincial Natural Science Foundation.

参考文献

[1] Dromey B, Zepf M, Gopal A, Lancaster K, Wei M, Krushelnick K, Tatarakis M, Vakakis N, Moustaizis S and Kodama R 2006 *Nature Physics* **2**, 456-459

[2] Wu W S, zhou Y K, Zhao S S and Yang Y J 2026 *Opt. Express* **34**, 16325-16341

[3] Yang Y J, Chen J G, Chi F P, Zhu Q R, Zhang H X and Sun J Z 2007 *Chin. Phys. Lett.* **24**, 1537-1540

[4] Qiao Y, Chen J Q, Zhou S S, Chen J G, Jiang S C and Yang Y J 2024 *Chin. Phys. Lett.* **41**, 014205

[5] Jiang W L, Qiao Y, Jiang s c, Zhou Y, Yang Y J and Chen J G 2025 *Phys. Rev. A* **112**, 023511

[6] Yuan G, Lu R, Jiang S and Dorfman K 2023 *Ultrafast Sci.* **3**, 0040

[7] Popmintchev T, Chen M C, Popmintchev D, Arpin P, Brown S, Aliauskas S, Andriukaitis G, Baliunas T, Mücke O D, Pugzlys A, Baltucka A, Shim B, Schrauth S E, Gaeta A, Hernndez-Garca C, Plaja L, Becker A, Jaron-Becker A, Murnane M M and Kapteyn H C 2012 *Science* **336**, 1287-1291

[8] Paul P M, Toma E S, Breger P, Mullot G, Auge F, Balcou P, Muller H G and Agostini P 2001 *Science* **292**, 1689-1692

[9] Krausz F and Ivanov M 2009 *Reviews of Modern Physics* **81**, 163-234

[10] Goulielmakis E, Schultze M, Hofstetter M, Yakovlev V S, Gagnon J, Uiberacker M, Aquila A L, Gullikson E, Attwood D T and Kienberger R 2008 *Science* **320**, 1614-1617

[11] Ishikawa T, Aoyagi H, Asaka T, Asano Y, Azumi N, Bizen T, Ego H, Fukami K, Fukui T and Furukawa Y 2012 *Nature Photonics* **6**, 540-544

[12] Miyamoto N, Kamei M, Yoshitomi D, Kanai T, Sekikawa T, Nakajima T and Watanabe S 2004 *Phys. Rev. Lett.* **93**, 083903

[13] Meyer M, Cubaynes D, Glijer D, Dardis J, Hayden P, Hough P, Richardson V, Kennedy E T, Costello J T and Radcliffe P *Phys. Rev. Lett.* **101**, 193002 (2008)

[14] Seipt D, Müller R, Surzhykov A and Fritzsche S 2016 *Phys. Rev. A* **94**, 053420

[15] Yuan H Y, Yang Y J, Guo F M, Chen J G, Wang J and Cui Z W 2024 *Phys. Rev. A* **109**, 2024

[16] Tian Y, Liu K and Zhou Y 2026 *Chin. Phys. B* **35**, 043203

[17] Cao Y, Shu Z, Tian D W and Hao X L 2026 *Chin. Phys. B* **35**, 064210

[18] Zhao Q, Peng Y, Che J, Chen C, Wang S, Xin G and Chen Y 2025 *Chin. Phys. B* **9**, 093201

[19] Gersten J I and Mittleman M H 1976 *J. Phys. B: At. Mol. Phys.* **9**, 2561

[20] Gavrila M and Kaminski J Z 1984 *Phys. Rev. Lett.* **52**, 613-616

[21] Kulander K C, Schafer K J and Krause J L 1991 *Phys. Rev. Lett.* **66**, 2601-2604

[22] Mihai G 2002 *J. Phys. B: At. Mol. Phys.* **35**, R147

[23] Liu H, Liu Y, Fu L, Xin G, Ye D, Liu J, He X T, Yang Y, Liu X, Deng Y, Wu C and Gong Q 2012 *Phys. Rev. Lett.* **109**, 093001

[24] X. Y. Lai, W. Quan, S. G. Yu, Y. Y. Huang and X. J. Liu 2018 *J. Phys. B: At. Mol. Phys.* **51**, 104003

[25] Morical T and Lin C D 2013 *Phys. Rev. A* **87**, 063405

[26] Boer M P de, Hoogenraad J H, Vrijen R B, Noordam L D and Muller H G 1993 *Phys. Rev. Lett.* **71**, 3263-3266

[27] Piraux B and Potvliege R M 1998 *Phys. Rev. A* **57**, 5009-5012

[28] Wei S S, Li S Y, Guo F M, Yang Y J and Wang B 2013 *Phys. Rev. A* **87**, 063418

[29] Demekhin P V and Cederbaum L S 2012 *Phys. Rev. Lett.* **108**, 253001

[30] Baghery M, Saalmann U and Rost J M 2017 *Phys. Rev. Lett.* **118**, 143202

[31] Jiang W C and Burgdörfer J 2018 *Opt. Express* **26**, 19921

[32] Su Q, Eberly J H and Javanainen J 1990 *Phys. Rev. Lett.* **64**, 862-865

[33] Pont M and Gavrila M 1990 *Phys. Rev. Lett.* **65**, 2362-2365

[34] Müller A D, Kutscher E, Artemyev A N, Cederbaum L S and Demekhin P V 2018 *Chem. Phys.* **509**, 145-150

[35] Zhou Z Y and Chu S I 2011 *Phys. Rev. A* **83**, 013405

[36] Yuan H Y, Yang Y J, Guo F M, Wang J, Chen J G, Feng W and Cui Z W 2023 *Opt. Express* **31**, 24213

[37] Arfken G B and Weber H J 1985 *Mathematical methods for physicists* 3rd ed.pp.701-707

[38] Schiff L I 1949 *A Textbook of Quantum Mechanics* (McGraw-Hill Book Company)

[39] Maung K M, Kahana D E and Norbury J W 1993 *Phys. Rev. D* **47**, 1182-1189

[40] Landau R H 1983 *Phys. Rev. C* **27**, 2191-2197

[41] Kwon Y R and Tabakin F 1978 *Phys. Rev. C* **18**(2), 932-943

[42] Yao G and Chu S I 1993 *Chem. phys. lett.* **204**, 381-388

[43] Zhou Z Y and Chu S I 2009 *Europhysics Letters* **88**, 17008

[44] Becker W, Grasbon F, Kopold R, Milošević D, Paulus G and Walther H 2002 *Adv. At., Mol., Opt. Phys.* **48**, 35-98